X-621-69-545

PREPRINT

NASA TM X-63795

EVIDENCE FOR STRONGLY DAMPED GRAVITY WAVES IN THE EARTH'S ATMOSPHERE

IGOR J. EBERSTEIN

DECEMBER 1969

GSFC

GODDARD SPACE FLIGHT CENTER
GREENBELT, MARYLAND

X-621-69-545

PREPRINT

EVIDENCE FOR STRONGLY DAMPED GRAVITY WAVES IN THE EARTH'S ATMOSPHERE

Igor J. Eberstein

Aeronomy Branch

December 1969

GODDARD SPACE FLIGHT CENTER

Greenbelt, Maryland

EVIDENCE FOR STRONGLY DAMPED GRAVITY WAVES IN THE EARTH'S ATMOSPHERE

Igor J. Eberstein*

Aeronomy Branch

ABSTRACT

Data from a series of pitot tube rocket soundings of the atmosphere are examined. The experiments consist of four soundings carried out over a two-day period at Fort Churchill, Canada in January and February 1967 by Smith, Theon and Horvath.

Temperature data from the four soundings were averaged, and a smooth curve was drawn through the points. A hydrostatically determined atmosphere based on the above lapse rate was calculated. Deviations from the above mean atmosphere were calculated, and a wavelike structure was observed. The waves grow very slowly below approximately 80 km, and acquire a more rapid growth rate at higher altitudes. The density and temperature variations have a wavelength of 10-20 km and appear to consistently be about 180 degrees out of phase. The pressure variation is somewhat irregular. However, in regions where pressure variation is well behaved it is out of phase with temperature and density by about 90 degrees.

Volland's theory of thermally damped gravity waves was used to compute wave patterns like those observed experimentally. A highly damped, upward propagating wave gives good results. Damping by conduction, turbulence and radiative transfer is examined, and turbulence is found to be the most important.

---

*NRC-NASA Research Associate

EVIDENCE FOR STRONGLY DAMPED GRAVITY WAVES IN THE EARTH'S ATMOSPHERE

I. EXPERIMENTAL EVIDENCE

Data from a series of pitot tube rocket experiments were studied. The experiments consisted of four soundings carried out over a two-day period at Fort Churchill, Canada in January and February 1967. The data are published by Smith et. al. (1967). The pitot tube technique is described by Horvath et. al. (1962).

The above experiments measure stagnation pressure with a pitot tube. The velocity and position of the vehicle are also determined. Density and temperature may then be determined by using the hydrostatic equation for the atmosphere and the ideal gas law. The underlying assumption of such a procedure is that vertical accelerations of air are small compared to the acceleration due to gravity. Present knowledge suggests that such an assumption is eminently reasonable.

The temperature data from the four soundings were averaged and a smooth curve drawn through the points, as shown in Figure 1. Admittedly, some arbitrariness is involved in drawing the mean temperature curve. However, such arbitrariness can only be satisfactorily resolved by reducing the scatter in the data. Such a reduction may be obtained by having more rocket shots in a series.

A hydrostatically determined atmosphere based on the above lapse rate was calculated. Experimental data were then plotted as $\rho/\bar{\rho}$, $P/\bar{P}$, $T - \bar{T}$ versus altitude where the barred quantities refer to the mean atmosphere calculated above. The four plots, figures 2-5, exhibit consistent behavior. Temperature and density appear to consistently be about 180 degrees out of phase. The density and temperature variations have a wavelength of 10-20 km. The pressure variation seems somewhat irregular. However, in the regions where pressure variation is well behaved it is out of phase with temperature and density variation by about 90 degrees. The waves grow very slowly below approximately 80 km, and acquire a more rapid growth rate at higher altitudes.

A correlation analysis was performed on the data below 80 km. Figure 6 shows auto-correlation plots for each of the four data sets individually, and for the four sets combined into one string of data. If the data is assumed to have a sinusoidal variation then the curve has the value 0.7 at $\lambda/8$, suggesting a wavelength of 12 km to 22 km with the mean at 16 km. If the variations are assumed to be random, then an integral scale of approximately 3.5 km is obtained. A power spectrum analysis of the combined density data was carried out, and is shown in Figure 7. The horizontal scale is wavelength and the vertical scale represents the spectral power density in arbitrary units. It is seen that wavelengths between 2 km and 16 km make a significant contribution, with a peak at 14 km. The analysis is not carried beyond 20 km wavelength since there is not enough data to justify such extension. For a discussion of correlation analysis and power spectra see Blackman and Tukey (1958), and Bendat and Piersol (1966).

II. GRAVITY WAVE THEORY

Waves in a stratified fluid under the influence of gravity appear to have been initially discussed by Burnside (1889) and Love (1891). Both authors treated an incompressible fluid. Görtler (1943) used schliierin photography to show experimentally that disturbances in an incompressible stratified medium under the influence of gravity propagate along characteristic rays. Lamb (1908) treated a compressible, adiabatic, ideal gas whose density is stratified by gravity. Since the original contributions by Burnside, Love and Lamb there have been many theoretical papers on various types of gravity waves. Reasonably up-to-date treatments of the subject may be found in Eckart (1960) and Yih (1965). However, gravity wave theory is currently undergoing an active phase of development and contributions are being added to the literature at a rapid rate.

The computer experiments to be discussed in this paper are based on a gravity wave theory developed by Volland (1969). Volland assumes an ideal gas which is conductive but inviscid. Volland had previously concluded (Volland, 1969, II) that, at least in the thermosphere, conductivity is more important as a damping mechanism than viscosity. In speaking of a conductive gas we shall mean a gas having an "effective conductivity," i.e., one in which a combination of thermal transfer processes behave in a manner which can be approximated by the heat conduction equation. Processes contributing to the effective conductivity include conduction, turbulent mixing, radiative transfer, and possibly chemical effects. The importance of these individual processes will be discussed below.

Since atmospheric gradients are usually gentle, the ray approximation for vertical wave propagation was used. Volland (1969, I) has shown that the ray treatment is a sufficient approximation for gravity waves propagating obliquely upwards, provided the horizontal wave number is in the order of, or greater than ω/a where a is the sound speed, and ω is the circular frequency of the wave. In the present study, the above condition was generally satisfied. The frequency of a moving fluid particle, or the 'intrinsic frequency' may be defined as

$$\Omega = \omega - \vec{k} \cdot \vec{U}$$

where

$\vec{k}$ is wave number

$\vec{U}$ is wind velocity

ω is wave frequency in a quiescent atmosphere

The above value of intrinsic frequency may be substituted into the equations describing gravity wave propagation in a quiescent atmosphere, and a solution obtained. Jones (1969) discusses the conditions under which the above procedure is valid. Basically, the following assumptions must be satisfied:

1. Vertical and horizontal derivatives of vertical winds must be less than $(N^2 - \Omega^2)^{1/2}$, where N is the Brunt-Vaisala frequency.
2. Horizontal derivatives of horizontal winds must be much smaller than Ω.

3. Time derivatives of horizontal winds must be much smaller than $(\Omega W/\beta) \cdot (N^2 - \Omega^2)^{1/2}$, where $\beta = N^2/g$.

4. Time derivatives of vertical winds are much smaller than g, the acceleration due to gravity.

These conditions are generally well met, except when Ω approaches either N or zero.

III. ESTIMATES OF EFFECTIVE CONDUCTIVITY

Processes contributing to "effective conductivity" include conduction, convection and turbulent mixing, radiative transfer and, possibly, chemical effects. The importance of these processes will now be considered. Conduction will be considered first.

Define:

$$\omega_h = \frac{\gamma C_p P}{2k}$$

where

γ = ratio of specific heats

C_p = specific heat capacity of air

k = conductivity of air

Further, define

$$G = \frac{\omega_h}{\omega}$$

where ω is the circular frequency of the gravity wave whose propagation is being considered. The above parameters are due to Volland (1969).

Now, the thermal diffusivity, κ, is defined as:

$$\kappa = \frac{k}{\rho C_p} .$$

Substituting into the equation for ω_h, one obtains:

$$\omega_h = \left(\frac{1}{2\kappa}\right)\left(\gamma \frac{P}{\rho}\right) .$$

The term in the second bracket is the formula for the square of the sound speed in an ideal gas. Thus one may write:

$$\omega_h = \frac{a^2}{2\kappa} .$$

Figure 8 shows a plot of ω_h versus altitude for the standard atmosphere. It is seen that ω_h, and therefore G, depend on density and temperature. Density variations of ±50% are readily observed, and similar variations in the damping parameters may be expected.

Though G decreases exponentially with increasing altitude, its value is everywhere quite large, compared with values of about 40,000 necessary to explain the slow upward wave growth which is observed. It is thus quite obvious that pure conduction does not provide an adequate damping mechanism, at least not below 120 km altitude.

The effects of conduction are generally enhanced by a combination of convection and turbulence.

Assume that we may define an effective turbulent thermal diffusivity K, such that

$$\frac{K}{\kappa} = \left(\frac{K}{\kappa}\right)_0 \left(\frac{Re - Re_{crit}}{Re_0}\right)$$

where κ is the molecular thermal diffusivity, and Re is Reynold's number. The Reynold's number is generally defined as follows:

$$Re = \frac{LV}{\nu}$$

where L is some suitable length dimension, V is a suitable velocity and ν is the kinematic viscosity. Following general astronomical practice, further justified by Blamont and DeJager (1961), L will be taken as the atmospheric scale height. Blamont and DeJager used a turbulent velocity, estimated from their measurements, for V. In the present study it will be assumed that

$$\tilde{V} = \beta \overline{V}$$

where $\tilde{V}$ the turbulent velocity, $\overline{V}$ is the mean wind velocity, and β is the ratio of r.m.s. turbulent fluctuation velocity to mean velocity of the flow, and is generally in the order of 10%. All that is necessary for the following discussion is that β remain approximately constant.

Blamont and DeJager (1961) found that the atmosphere undergoes a turbulent to laminar transition at about 100 km altitude. At this point, the Reynold's number based on fluctuation velocity is 2,000.

In the present study a mean wind structure having the following characteristics is assumed:

$$V = \sqrt{Z} \qquad 0 \leq Z \leq 5$$

$$V = Z \qquad Z \geq 5$$

where V is mean wind speed in meters per second, and Z is altitude in kilometers. The mean velocity is then used to calculate the Reynold's number, resulting in a transition Re of 20,000. This result agrees with Blamont, and DeJager's value if one substitutes $\tilde{V} = 0.1\,\bar{V}$.

Experimental data presented in the Meteorological Rocket Network Data Reports (1967), and the upper atmosphere wind measurements of Bedinger (1968) show that the assumed wind profile is reasonable. However, it must be realized that winds have great temporal variability, and therefore, any stationary model must be accepted with great caution. The wind variability of course suggests great variability in the turbulence level, and therefore, variations in the damping factor.

The reference value K_0 was taken from early Eiffel tower measurements reported by Brunt (1952) for an altitude of some 150 meters. There, $K_0 = 10^5$ cm^2/sec. Since κ_0 is 0.2 cm^2/sec, the ratio, $(K/\kappa)_0 = 5 \times 10^5$.

Figure 9 shows K/κ versus altitude. The two triangles represent K^1/D where K^1 is turbulent mass diffusivity, and D is molecular diffusivity. The mass transfer data are from the work of Booker (1956) and Zimmerman and Champion (1963). The agreement is seen to be reasonable. Zimmerman and Champion's results also show approach to molecular behavior around 100 km altitude, in agreement with the results of Blamont and DeJager.

Figure 8 shows ω_h based on turbulent heat transport versus altitude. Turbulent transport of chemically active species may further enhance the effective conductivity.

Another contributor to effective conductivity is radiative transfer. Brunt (1952) showed than when photon mean path is short compared to a representative length, the radiative energy transport behaves in a manner similar to conduction, and may be treated by means of a conductivity equation. Brunt's conclusion is what one would expect from the physical nature at the two processes, i.e., energy transfer by a molecular random walk is quite similar to energy transfer by a photon random walk. In both cases the mean free path must be small compared to a relevant physical dimension. For the region where water vapor absorption is important Brunt estimated a radiative diffusivity coefficient $K_p \simeq 1.3 \times 10^3$ cm^2/sec. The radiative diffusivity based on carbon dioxide absorption will, of course, be smaller.

Let us examine some of the properties of radiative diffusivity based on carbon dioxide. Elsasser and Culbertson (1960) review experimental data on

CO_2 absorption and conclude that below one atmosphere total pressure the low resolution absorption is relatively independent of total gas pressure, depending only on the amount of absorber gas. The mixing ratio of CO_2 in the atmosphere is approximately constant. The radiative conductivity is

$$X_r = b\bar{\alpha}$$

where $\bar{\alpha}$ is mean absorption coefficient, and

$$\bar{\alpha} = \rho\bar{\alpha}_0 .$$

The radiative thermal diffusivity is defined as

$$K_R = \frac{X_r}{\rho C_p} .$$

It follows that

$$K_R = \frac{\rho\bar{\alpha}_0}{\rho C_p} = \frac{\bar{\alpha}_0}{C_p}$$

and is approximately constant throughout the atmosphere, provided the radiative properties themselves do not significantly change.

Radiative transfer due to water and ozone are, of course, altitude dependent.

Golitsyn (1963) studied radiative damping of waves for long photon mean path. Golitsyn developed a coefficient of radiative conductivity given by:

$$X_R = 4\pi \int_0^{\infty} \frac{\alpha_\nu}{k} \frac{dB_\nu}{dT} \left(\frac{\alpha_\nu}{k} \arctan \frac{k}{\alpha_\nu} - 1 \right) \frac{d\nu}{k}$$

where ν is wave number of the radiation, and k is wave number of the gasdynamic disturbance. α_ν is the frequency dependent absorption coefficient, and B_ν is the Planck function.

Damping by carbon dioxide and ozone were studied, using low resolution absorption spectra given by Elsasser and Culbertson (1960). The results are shown in Figure 8. It is seen that for the longer vertical wavelengths radiation damping does become significant. However, the damping estimate in the band center is likely to be somewhat high for the longer wavelengths since there the mean photon path is not really long compared to the wavelength of the gravity wave. When the mean photon path is not long, then Golitsyn's formula tends to overestimate the attenuation. However, the mean photon path for shorter gravity waves as well as in the wings of the band for all wavelengths is long and a correct damping estimate may be expected. Atmospheric ozone distributions were taken from Mitra (1952) and Krueger (1969).

In conclusion it may be said that turbulent heat transport is the most important damping mechanism with radiation making a significant contribution below 75 km. Above 110 km, conduction provides most of the damping.

IV. NUMERICAL CALCULATIONS

The numerical calculations were based on the gravity wave treatment developed by Volland (1969). Essentially, Volland uses a matrix method to obtain periodic solutions of a linearized version of the following set of equations:

$$\frac{\partial \rho}{\partial t} + \nabla \cdot (\rho \vec{v}) = 0$$

$$\rho \frac{D\vec{v}}{Dt} + \nabla P - \rho \vec{g} = 0$$

$$\rho C_v \frac{DT}{Dt} + P \nabla \cdot \vec{v} - \nabla(\kappa \nabla T) = 0$$

$$P - \mu \rho T = 0$$

Inclusion of the heat transfer term in the energy equation provides a mechanism of dissipation since destruction of thermal gradients leads to the creation of entropy.

Solution of the linearized equations yields a dispersion relation which may be solved for the vertical wave number giving:

$$k_z = k_0 \sqrt{\frac{\gamma}{2} - A^2 - S^2 - iG \pm \sqrt{D}}$$

where

$$D = \left(\frac{\gamma}{2} - iG\right)^2 + 2iG\left(1 + B^2 S^2\right)$$

ω = circular frequency of the wave

a local sound speed

k_0 = ω/a

γ = ratio of specific heats

ω_B = $g/a\sqrt{\gamma - 1}$ = Brunt - Vaisala frequency

ω_A = $\gamma g/2a$ = $a/2H$

g = acceleration due to gravity

H = Pressure scale height

A = ω_A/ω

B = ω_B/ω

S = k_x/k_0

G = ω_h/ω

ω_h = $a^2/2\kappa$

κ = thermal diffusivity

The adiabatic case is obtained in the limit as G becomes infinite. In that situation the dispersion relation becomes the same as obtained by Hines (1960), i. e.

$$n_z^2 = \left\{1 - \left(\frac{\omega_A}{\omega_B}\right)^2\right\} - n_x^2 \left\{1 - \left(\frac{\omega_B}{\omega}\right)^2\right\}$$

where

$$n_x = \frac{k_x a}{\omega} \qquad n_z = \frac{k_z a}{\omega} .$$

Georges (1967) has shown that the dispersion equation may be rearranged into the form

$$\frac{k_x^2}{\ell^2} + \frac{k_z^2}{m^2} = 1$$

where

$$\ell^2 = \frac{\omega^2 - \omega_A^2}{a^2\left(1 - \frac{\omega_B^2}{\omega^2}\right)}$$

and

$$m^2 = \frac{\omega^2 - \omega_A^2}{a^2} .$$

As $\omega \to \infty$

$$\ell^2 = m^2 = \frac{\omega^2}{a^2}$$

giving:

$$\left(\frac{k_x a}{\omega}\right)^2 + \left(\frac{k_z a}{\omega}\right)^2 = 1$$

$$k_x^2 + k_z^2 = \frac{\omega^2}{a^2}$$

$$k = \frac{\omega}{a}$$

i.e., the two-dimensional equation for a pure sound wave.

Conversely, as $\omega \to 0$

$$\ell^2 \to \left(\frac{\omega}{a}\right)^2 \left(\frac{\omega_A}{\omega_B}\right)^2$$

$$m^2 \to -\left(\frac{\omega}{a}\right)^2 \left(\frac{\omega_A}{\omega}\right)^2$$

giving

$$k_z^2 = \left(\frac{\omega_B}{\omega}\right)^2 k_x^2 - \frac{1}{4H^2}$$

where use was made of the equality

$$\frac{\omega_a}{a} = \frac{1}{2H} .$$

The low frequency limit dispersion equation is very close to what would be obtained by using an incompressible, density stratified atmosphere with gravity

Tolstoy (1963) cited by Georges (1967), gives:

$$k_z^2 = k_x^2 \left(\frac{\omega_B^2}{\omega^2} - 1\right) - \frac{1}{4H^2} .$$

For small ω the Tolstoy formula becomes identical with the low frequency dispersion relation derived above.

For $\infty > \omega > \omega_A$ the regime may be viewed as one of acoustic waves modified by the influence of gravity. Clearly the gravitational influence will be most strongly felt for low frequency "infrasonic" waves.

For $\omega_B > \omega > 0$ the regime may be viewed as one of gravity waves modified by the effects of compressibility.

Continuing the above form of resoning, the Volland dispersion relation represents a compressible gravity wave modified by heat transfer.

Originally a plane wave solution was assumed, and shown to be compatible with the linearized equations. One may solve for the physical parameters to obtain what Hines (1960) has called polarization relations. The physical parameters may then be written in matrix form as

$$(e) = (K)(c)$$

where

$$(e) = \begin{pmatrix} e_1 \\ e_2 \\ e_3 \end{pmatrix}$$

is the matrix of physical parameters with

$$\frac{w}{a} = e_1 \delta$$

$$\frac{\Delta P}{P} = e_2 \delta \qquad \frac{\Delta T}{T} = e_3 \delta$$

$$\frac{\Delta \rho}{\rho} = (e_2 - e_1) \delta$$

$$\frac{u}{a} = e_2 \frac{S\delta}{\gamma}$$

where

$$\delta = \frac{1}{\sqrt{a\bar{\bar{p}}}}$$

is an altitude normalization factor.

w is vertical perturbation velocity

u is horizontal pertubation velocity

c is the "basic wave"

$$c = c_0 \exp\left[i\left(\omega t - k_z z - k_x x\right)\right].$$

Taking the wave at t = 0, x = 0, one obtains

$$c = c_0 e^{k_z z}$$

for an isothermal atmosphere.

The ray solution for a series of isothermal slabs then gives

$$c = c_0 \exp\left[-ik_0 \int_{z_0}^{z} q(\xi)\, d\xi\right].$$

where

$$q = \frac{k_z}{k_0}$$

The transformation, or polarization, matrix K is given by:

$$K = \begin{pmatrix} L_1 \\ L_2 \\ L_3 \end{pmatrix}$$

where

$$L_1 = q - iA\left\{1 - \frac{2S^2}{\gamma}\right\}$$

$$L_2 = \gamma - 2A^2 - 2i\,Aq$$

$$L_3 = \gamma - S^2 - A^2 - q^2$$

The above matrix of Volland (1968) reduces to Hines' (1960) polarization relations for the adiabatic case.

A mean temperature profile was fed into the computer program which then calculated a mean atmosphere and various characteristic quantities based on the mean atmosphere at 1 km vertical intervals. The atmosphere was assumed to be homogeneous horizontally. The mean atmosphere was based on the hydrostatic equation and the ideal gas law.

Values of the circular frequency, ω, and the horizontal wavelength were selected. The range of frequencies considered was 10^{-3} sec to 10^{-2} sec. The horizontal wavelength, λ_x was varied between 25 km and 500 km.

The initial amplitude of the elementary wave was adjusted to match the density deviation in the 20 km to 40 km altitude region.

A series of values of the damping parameter G were selected. A fairly high value of damping was found to be necessary to give a wave growth comparable to what was observed experimentally.

Most calculations were for a quiescent atmosphere, but several wind distributions were also studied. A wind which varied sinusoidally with altitude was found to give the most interesting results.

V. DISCUSSION OF RESULTS

Figure 10 shows density fluctuation for a series of gravity waves, the first two of which have damping characteristics shown in Figure 8. The third curve has the same variation of damping coefficient with altitude, only damping is twice as large as in the previous two cases. Figure 11 shows a situation where the value of G is kept constant at 40,000. For the value of omega chosen (9×10^{-4} sec^{-1}) the above implies ω_H = 36 sec^{-1} = constant, i. e. approximately twice as much damping as estimated in Figure 8. Figure 12 shows the situation where the damping coefficient increases linearly with altitude, and $G = G_0/Z$

where Z is altitude in km, $G_0 = 940{,}000$. For $\omega = 9.0 \times 10^{-4}\ sec^{-1}$. $\omega_H = 18\ sec^{-1}$ at 50 km and $8.5\ sec^{-1}$ at 100 km. These values imply an order of magnitude more damping than estimated. Whereas the damping estimate could be too low, it is more likely to be on the high side. Thus, different explanations are called for. It is also unlikely that contributions from viscosity effects would be an order of magnitude more significant than the thermal effects. Two alternatives remain. Either the damping is due to non-linear terms not considered in the theory, or additional turbulence is generated by the gravity waves, so that eventually the waves are propagating into a turbulence field which is much stronger than the mean field existing in the absence of gravity wave activity. Such a conclusion is eminently reasonable, considering that a gravity wave having a 30% density deviation generates a wind well over 100 m/sec.

Gossard (1962) observed gravity waves in the troposphere. He found the period to vary between 15 minutes and 2 hours. The horizontal wavelength for waves of 15 minute period was 19 km and for waves of 2 hours period it was 150 km. The periods investigated in the present study range from 19.5 minutes to 1.94 hours, thus being approximately the same as those observed by Gossard. However, the horizontal wavelength range was between 372.5 km and 48.5 km, i.e., about 2.5 times the wavelengths reported by Gossard. The difference is due to the longer vertical wavelengths which are indicated by the present study. Quite approximately

$$\frac{\lambda_z}{\lambda_x} \sim \frac{\omega}{\omega_B}$$

Thus, for a given atmosphere and period the vertical wavelength is approximately proportional to the horizontal wavelength, and a larger vertical wavelength calls for a larger horizontal wavelength.

The sinusoidal background wind field shown in Figure 12 results in considerable modulation of the gravity wave. The modulation is of the same type as observed in the experiments, only more pronounced.

The winds correspond to typical conditions both as regards amplitude and wavelength. Figure 13 shows an experimental wind pattern obtained at Fort Churchill by Smith et al. (1965).

CONCLUSIONS

Semi-quantitative agreement between an atmospheric wavelike structure and gravity wave theory has been demonstrated. Also, the study indicates what further experiments will be needed to close the loopholes in our understanding.

The most important damping mechanism is turbulence. However, naturally occurring turbulence does not appear adequate to provide the experimentally required damping. It is suggested that gravity wave activity creates its own, much stronger turbulence field. Thus it would be important to measure atmospheric turbulence both at times of low and high gravity wave activity.

Modulation of the wave by the wind field is important. Thus, it would be important to simultaneously measure the thermodynamic parameters and the background windfield.

APPENDIX A

The following contains some further thoughts on turbulent damping. In Figure 14, samping estimates by various authors are shown.

Hosler (1969) determined vertical diffusivity from radon profiles. Average derived vertical diffusivities for a 90 meter height interval range from about 3.1×10^5 cm^2/sec during unstable convective periods to about 8.3×10^3 cm^2/sec during stable inversion periods. The above measurements were carried out at a tower site near Washington, D. C. The Eiffel tower measurements reported by Brunt, and discussed in the main text, gave 10^5 cm^2/sec which is close to Hosler's value for unstable convective periods.

The estimates of Johnson and Wilkins (1965, 1966) are based on estimated limits of steady downward heat transport in the atmosphere. Colegrove, Johnson and Hanson (1966) estimate an average eddy diffusion coefficient based on molecular and atomic oxygen transport.

The experimental damping curve shows the amount of damping necessary to maintain the observed growth rate of gravity waves with altitude. It is seen that the needed damping is considerably greater than any steady state estimates. However, the experimental damping estimates are below the diffusion coefficients determined by Hodges (1969) for a gravity wave where amplitude does not increase with altitude.

REFERENCES

Bendat, J. S. and A. G. Piersol (1966), "Measurement and Analysis of Random Data", Wiley, New York.

Bedinger, J. F. "Investigation of Temporal Variations of Winds", GCA Corp, Bedford, Mass., December, 1968.

Blackman, R. B. and J. W. Tukey, (1958), "The Measurement of Power Spectra", Dover.

Blamont, J. E. and C. DeJager, "Upper Atmosphere Turbulence near the 100 km Level" Annales de Geophysique., (1961), pp. 134-144.

Booker, H. G. "Turbulence in the Ionosphere with Applications to Meteor Trails, Radio-Star Scintillation, Auroral Radar Echoes, and Other Phenomena". J. Geophys. Res. Vol. 61, pp. 673-705 (December, 1956)

Brunt, D. "Physical and Dynamical Meteorology", Cambridge, University Press, 1952, p. 229.

Burnside, W. "On the Small Wave-Motion of a Heterogeneous Fluid Under Gravity", Proc. London Math. Soc. (1889), pp. 392-397.

Colegrove, F. D., F. S. Johnson and W. B. Hanson, "Atmospheric Composition in the Lower Thermosphere", J. Geophys. Res., Vol. 71, (May 1966), pp. 2227-2236.

Eckart, Carl (1960), "Hydrodynamics of Oceans and Atmospheres", New York, Pergammon.

Elsasser, W. M. with Culbertson, M. F. "Atmospheric Radiation Tables", Meteorological Monographs, Vol. 4, No. 23, August, 1960.

Georges, T. M. "Ionospheric Effects of Atmospheric Waves", ESSA Tech. Rep. IER 57-ITS-A54, pp. 28-68, 1967.

Golitsyn, G. S., "The Influence of Radiative Transfer on the Propagation of Sound in the Atmosphere", Bull (Izv), Academy of Sciences, USSR, Geophys. Ser. No. 6, 1963.

Gossard, E. E. "Vertical Flux of Energy into the Lower Ionosphere from Internal Gravity Waves Generated in the Troposphere", J. Geophys. Res. Vol. 67, No. 2 (February, 1962), pp. 745-757.

Görtler, H. (1943), "Uber eine Schwingungserscheinung in Flüssigkeiten mit stabiler Dichteschichtung". Zeitscheift für Angewandte Mathematik und Mechanik. Band 23, Heft 2, pp. 65-71.

Hines, C. O. "Internal Atmospheric Gravity Waves at Ionospheric Heights", Can. J. Phys. 38, 1441-1481, 1960.

Hodges, R. R. "Eddy Diffusion Coefficients due to Instabilities in Internal Gravity Waves", J. Geophys. Res., Vol. 74.

Horvath, J. J., Simmonds, R. W. and Brace, L. H. (1962), "Theory and Implementation of the Pitot-Static Technique for Upper Atmospheric Measurements", Space Physics Res. Lab. Scientific Report NS-1, Univ. of Michigan, March, 1962.

Hosler, C. R. "Vertical Diffusivity from Radon Profiles", J. Geophys. Res., Vol. 74, (Dec. 1969) pp. 7018-7026.

Johnson, F. S. and Wilkins, E. M. Correction to 'Thermal Upper Limit on Eddy Diffusion in the Mesosphere and Lower Thermosphere', J. Geophys. Res., Vol. 70, (Aug. 1966) p. 4063.

Jones, W. L. "Ray Tracing for Internal Gravity Waves," J. Geophys. Res. Vol. 74, pp. 2028-2033, April, 1969.

Krueger, A. J. "Rocket Measurements of Ozone over Hawaii," Ann. Geophys. T. 25, fasc. 1, 1969, p. 307 a 311.

Krueger, A. J. Personal Communication, Goddard Space Flight Center, Greenbelt, Maryland, November, 1969.

Lamb, H. "On the Theory of Waves Propagated Vertically in the Atmosphere", Proc. London Math. Soc. (1909) pp. 122-141.

Love, E. H. "Wave-Motion in a Heterogeneous Heavy Liquid" Proc. London Math. Soc. (1891), pp. 307-316.

Meteorological Rocket Network Firings Data Report, January, 1967.

Mitra, S. K. "The Upper Atmosphere" Calcutta, The Asiatic Society, 1952, pp. 130-140.

Smith, W. S., Theon, J. S., Swartz, P. C. and Katchen, L. B. "Temperature, Pressure, Density and Wind Measurements in the Upper Stratosphere and Mesosphere", 1965, NASA TR R-263.

Smith, W. S., Theon, J. S., Swartz, P. C., Casey, J. F. and Horvath, J. J. (1964), "Temperature, Pressure, Density, and Wind Measurements in the Stratosphere and Mesosphere", 1967 NASA TR R-316.

Tolstoy, I. "The Theory of Waves in Stratified Fluids Including the Effects of Gravity and Rotation" Rev. Mod. Phys. 35, 207-230, 1963.

Volland, H. (1969, I) "Full Wave Calculation of Gravity Wave Propagation through the Thermosphere", J. Geophys. Res. Vol. 74, pp. 1786-1795, April 1969.

Volland, H. (1969 II) "The Upper Atmosphere as a Multiply Refractive Medium for Neutral Air Motions", J. Atmospheric and Terrestial Physics, 1969 (to be published).

Yih, Chia-Shun (1965) "Dynamics of Non-Homogeneous Fluids", New York, Macmillan.

Zimmerman, S. P. and Champion, K. S. W. "Transport Processes in the Upper Atmosphere", J. Geophys. Res., Vol. 68, pp. 3049-3056, May, 1963.

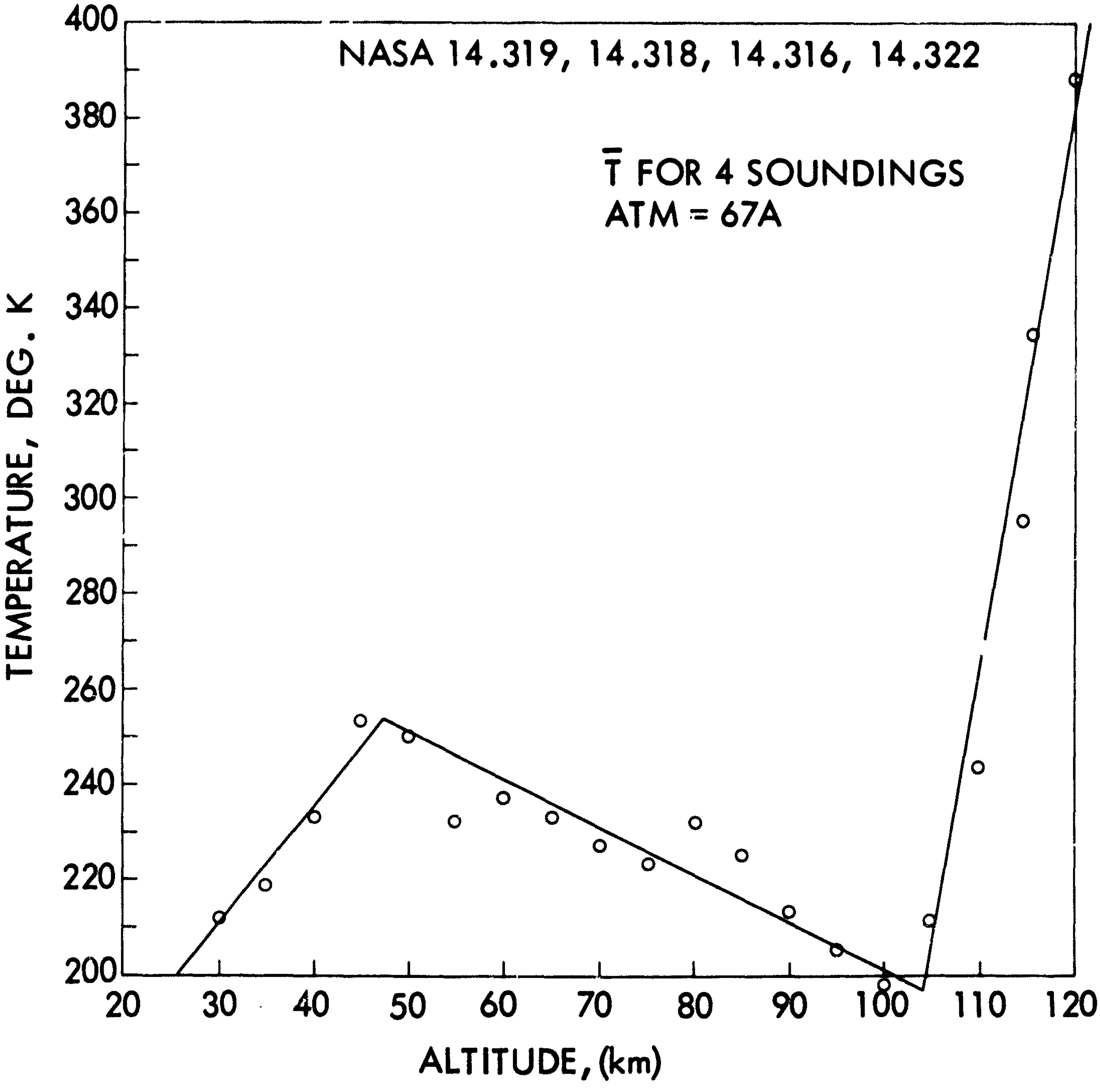

Figure 1. Mean Temperature Fro.n Four Rocket Soundings

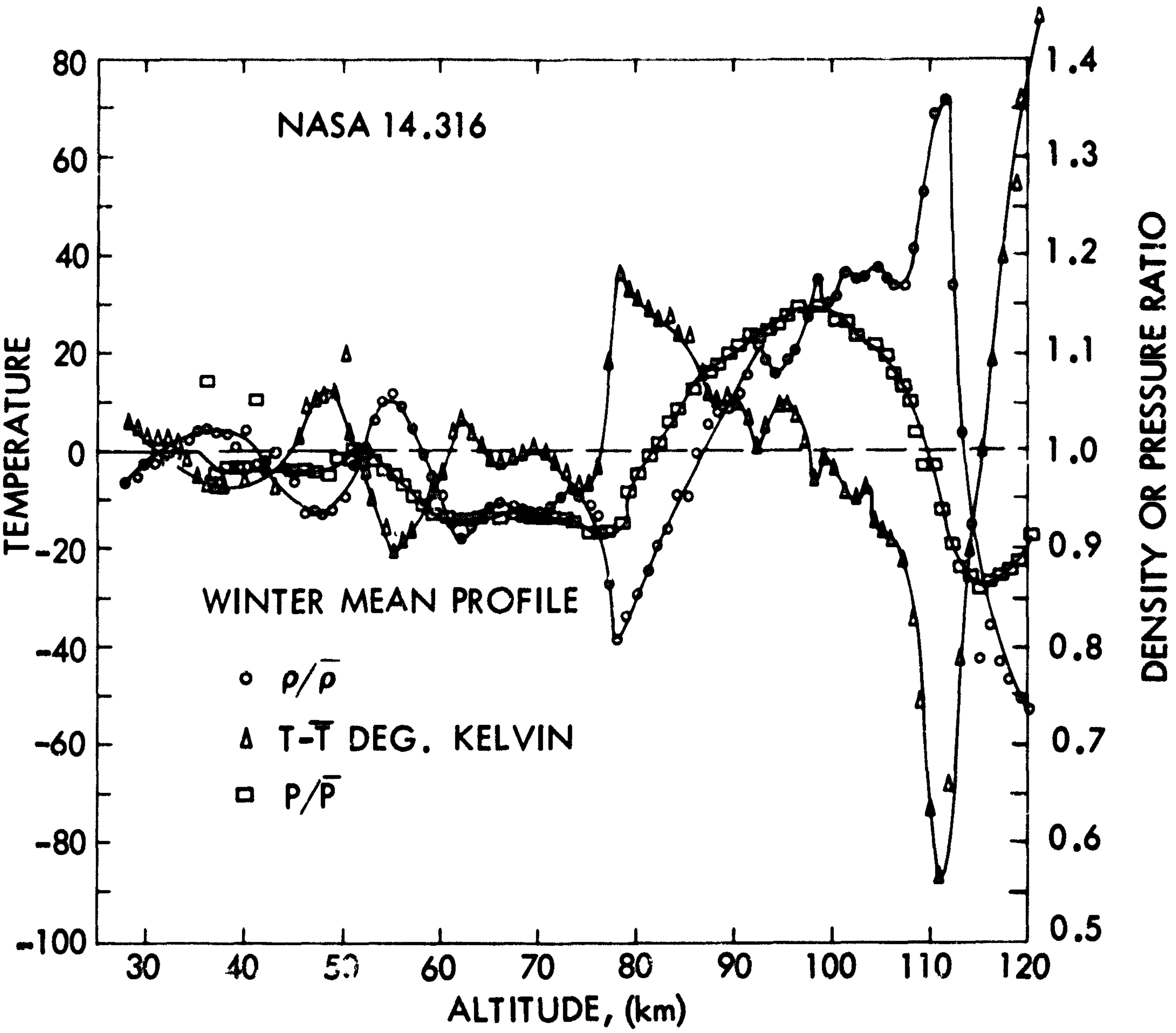

Figure 2. Deviation of Atmospheric Density, Pressure, and Temperature From The Mean

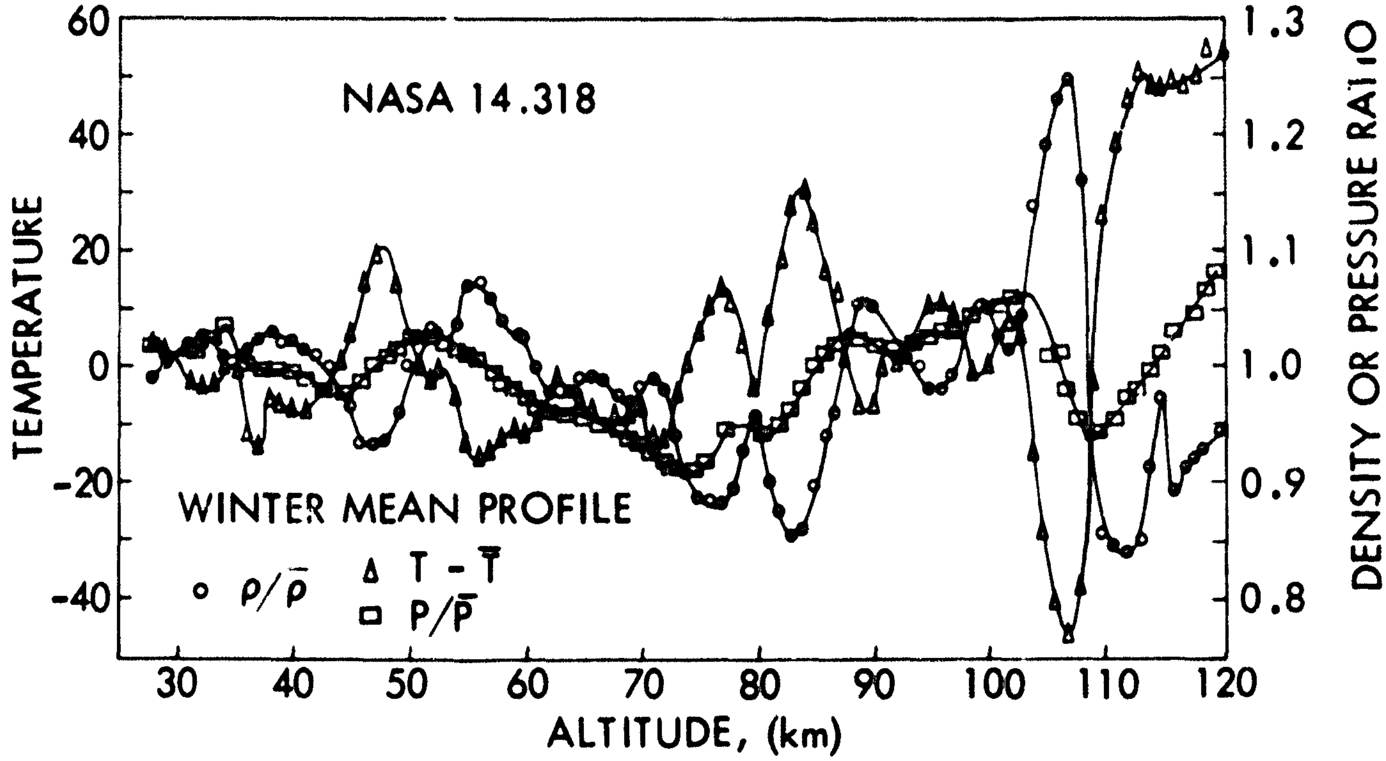

Figure 3. Deviation of Atmospheric Density, Pressure, and Temperature From The Mean

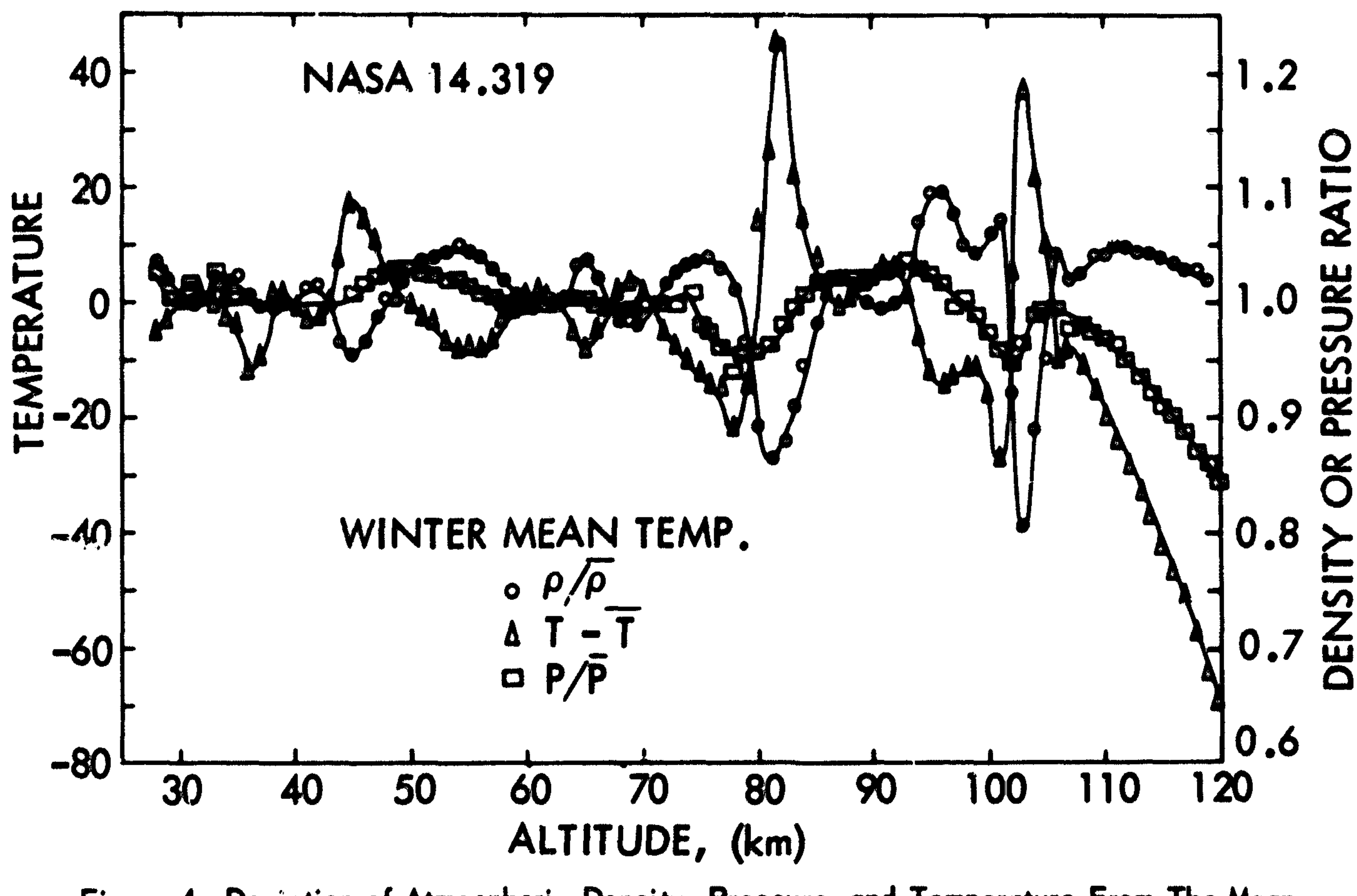

Figure 4. Deviation of Atmospheric Density, Pressure, and Temperature From The Mean

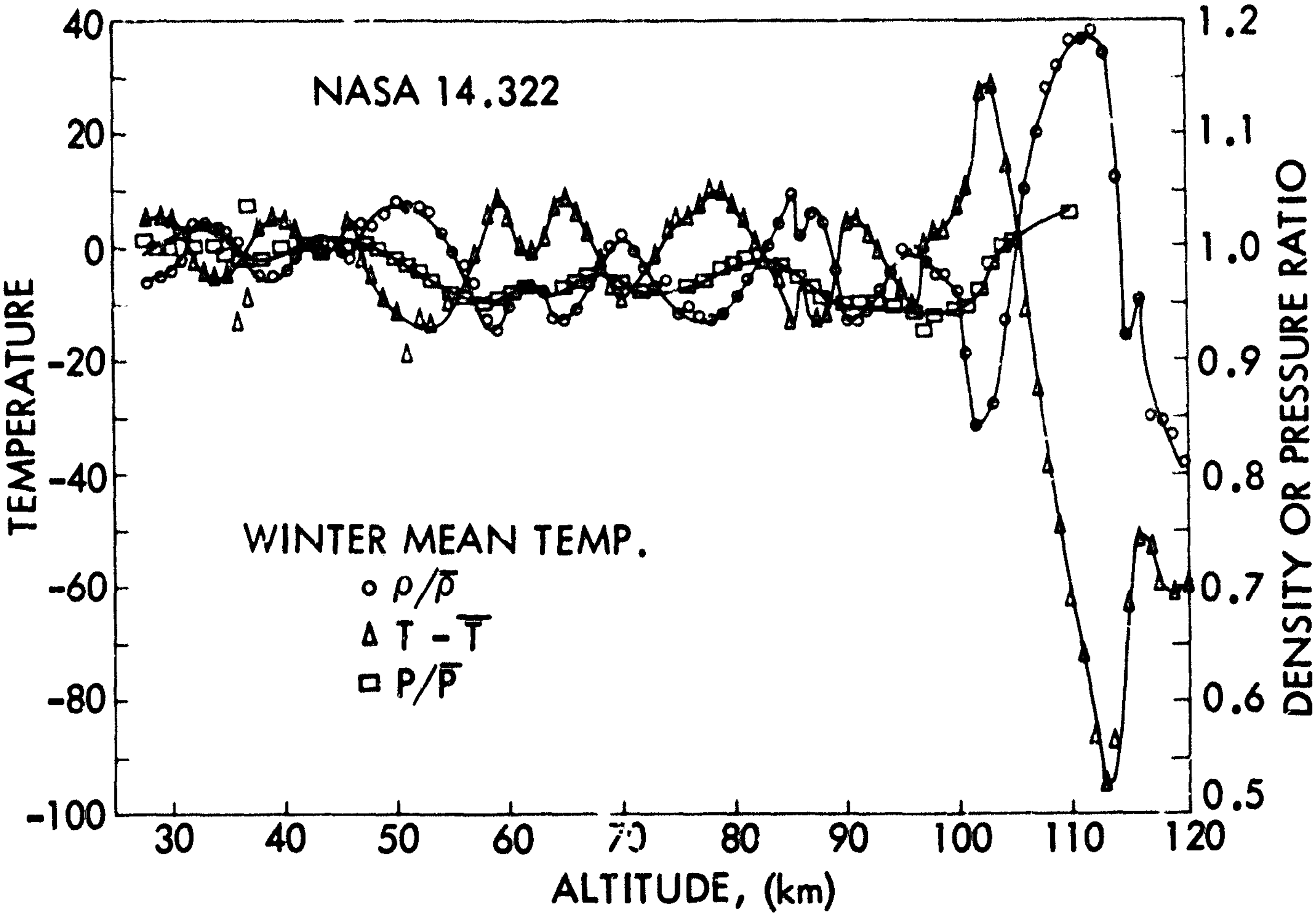

Figure 5. Deviation of Atmospheric Density, Pressure, and Temperature From The Mean

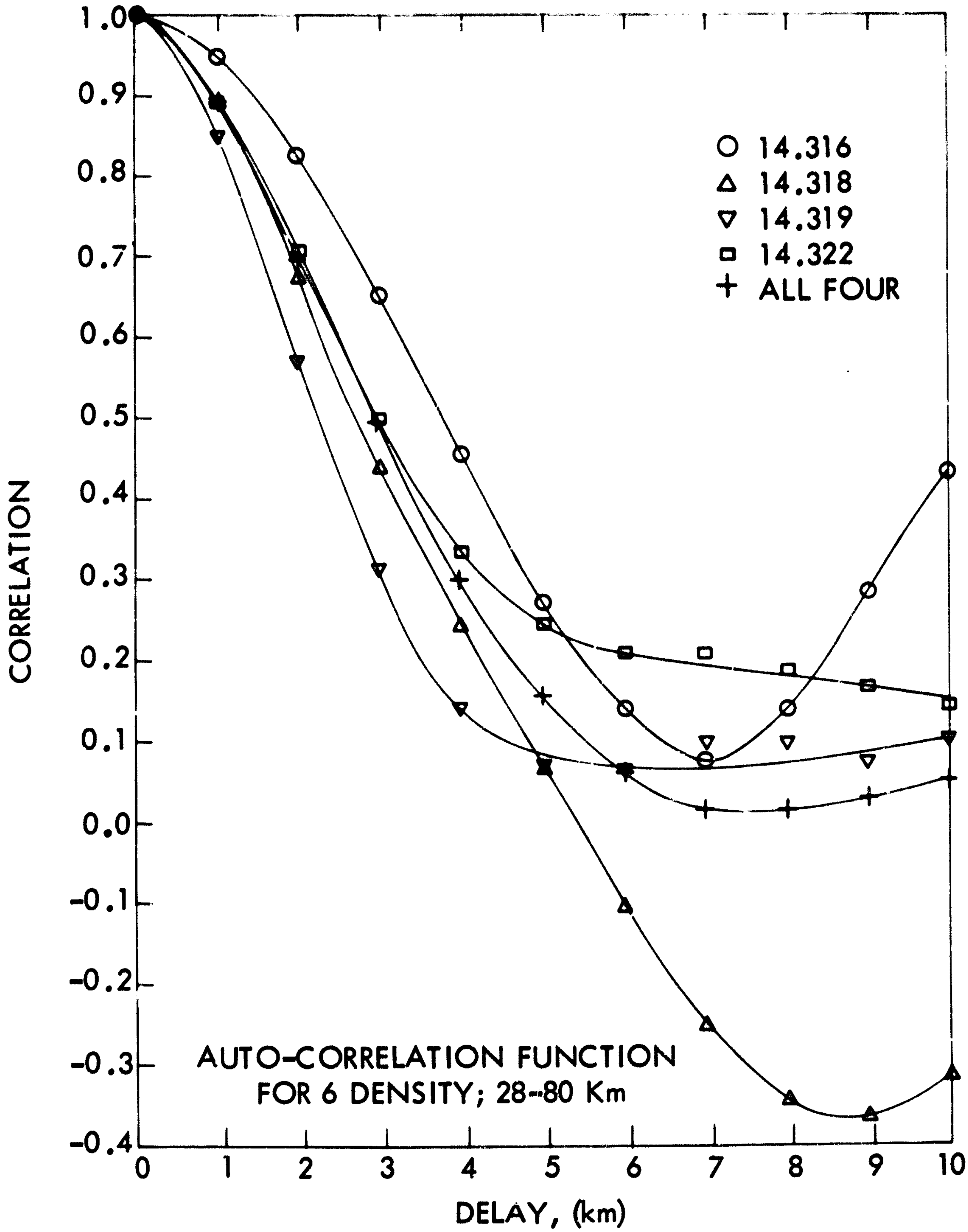

Figure 6. Spatial Auto-Correlation Function For Atmospheric Density

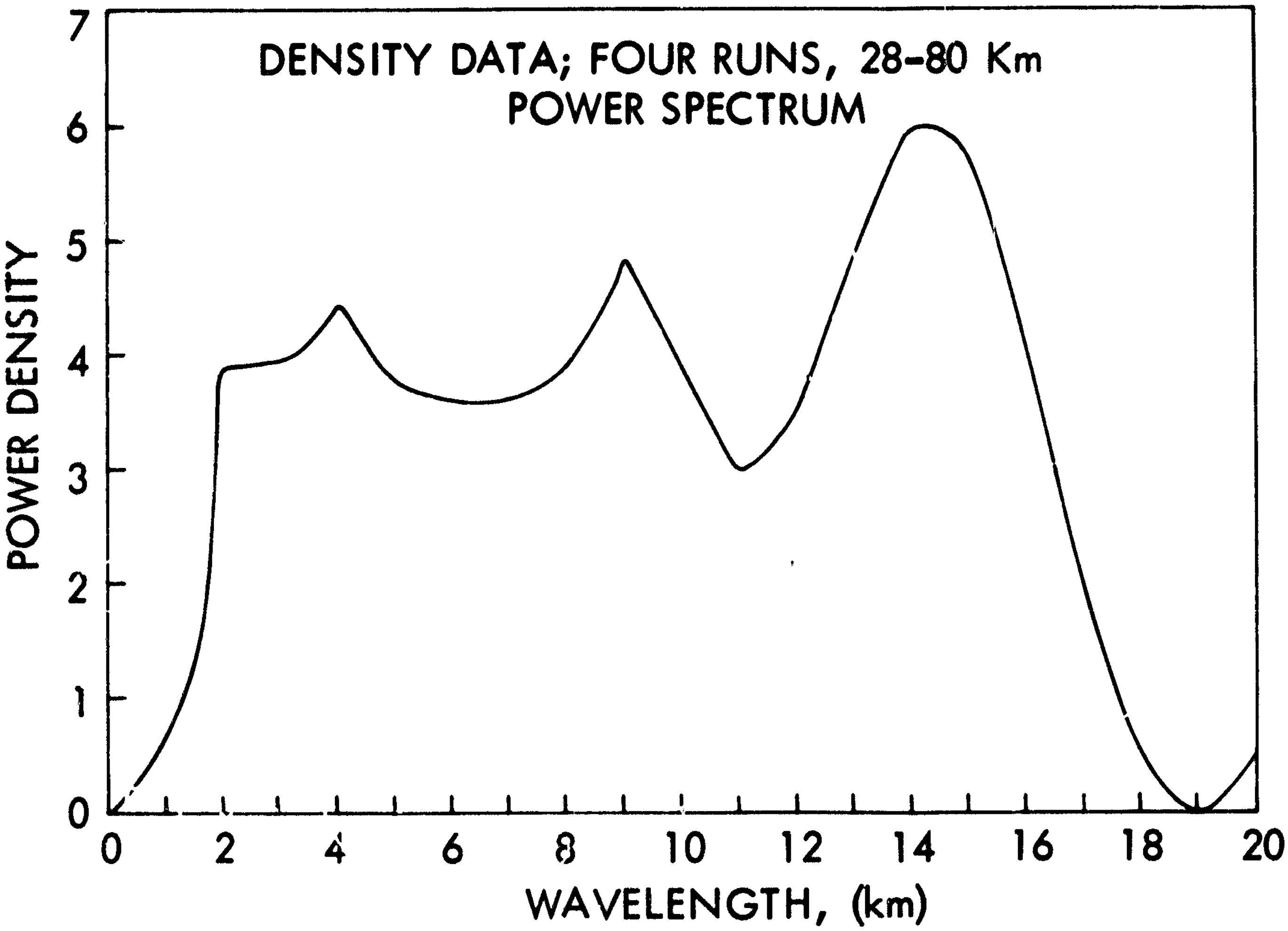

Figure 7. Spatial Power Spectral Density For Atmospheric Density Deviation

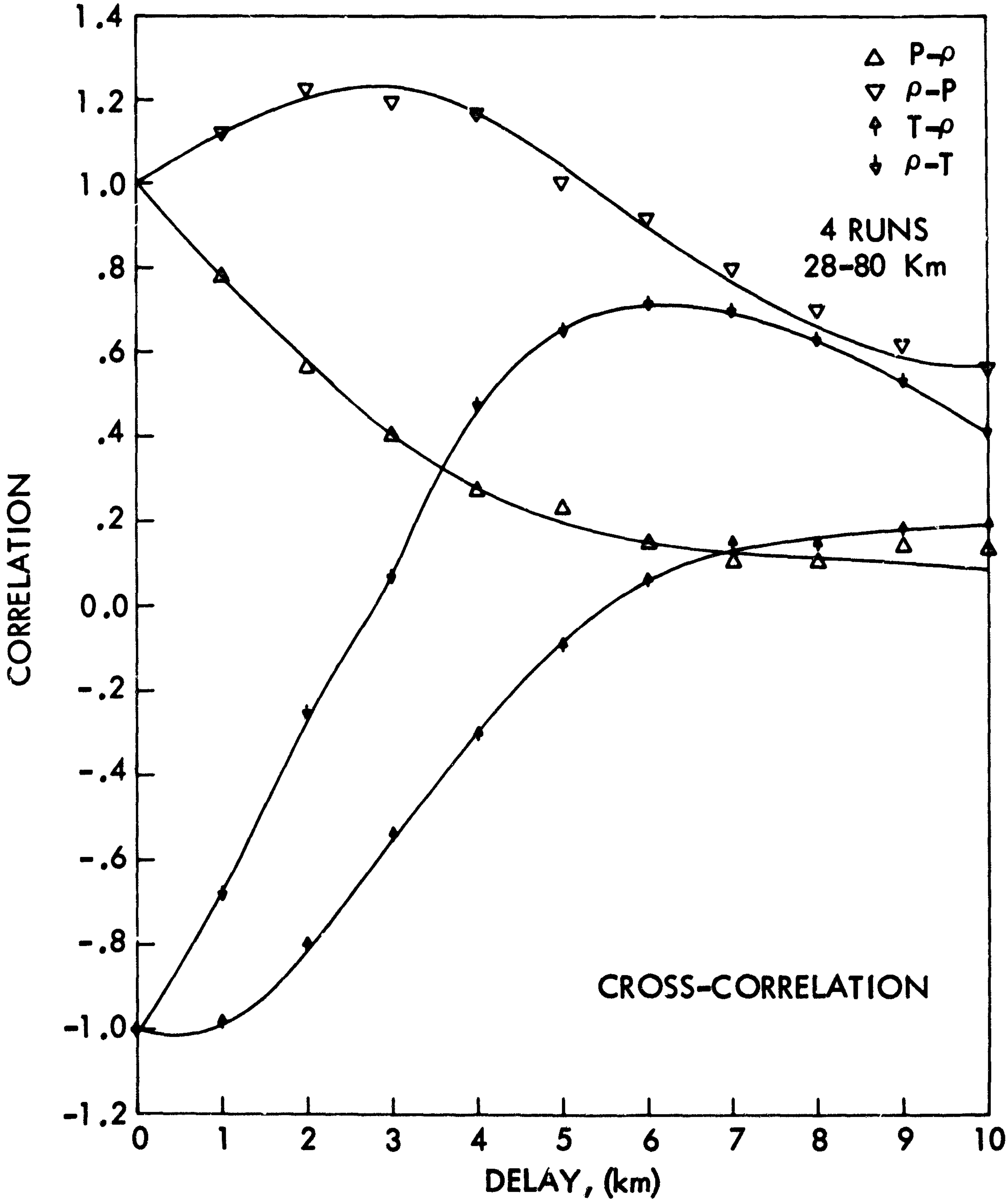

Figure 8. Spatial Cross Correlation Functions

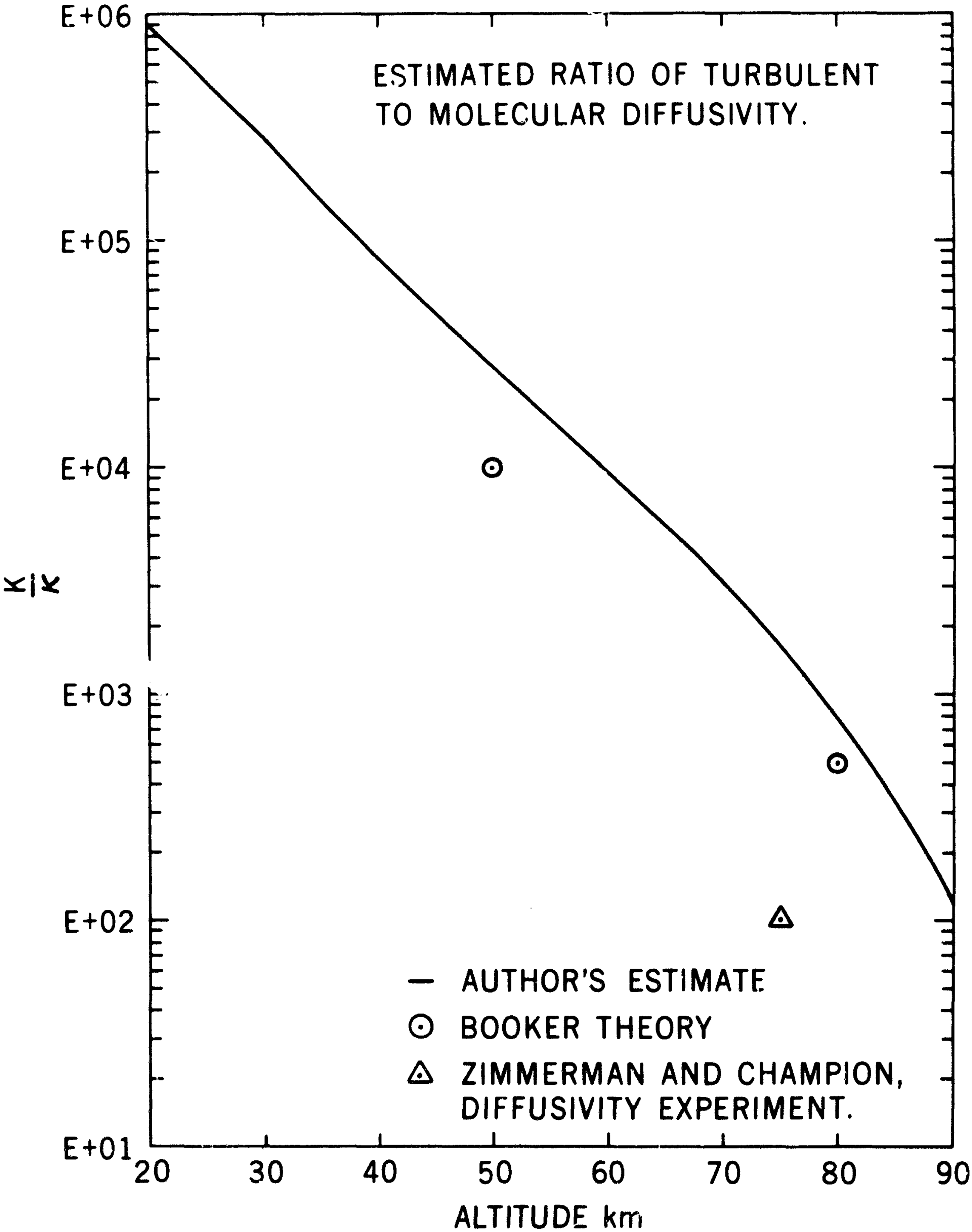

Figure 9. Estimated Ratio Of Turbulent To Molecular Diffusivity As A Function Of Altitude

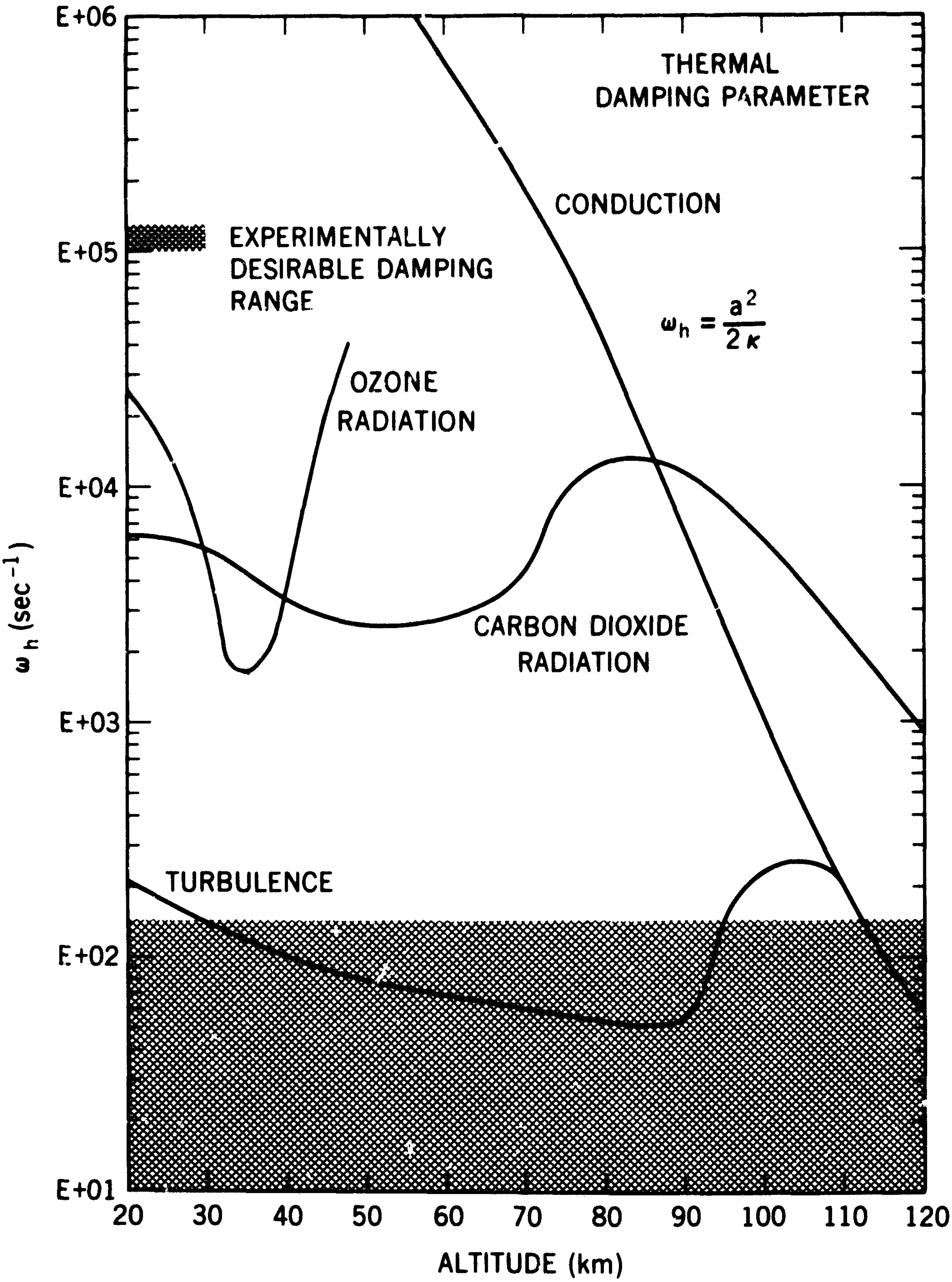

Figure 10. Damping Parameter, G, As A Function Of Altitude

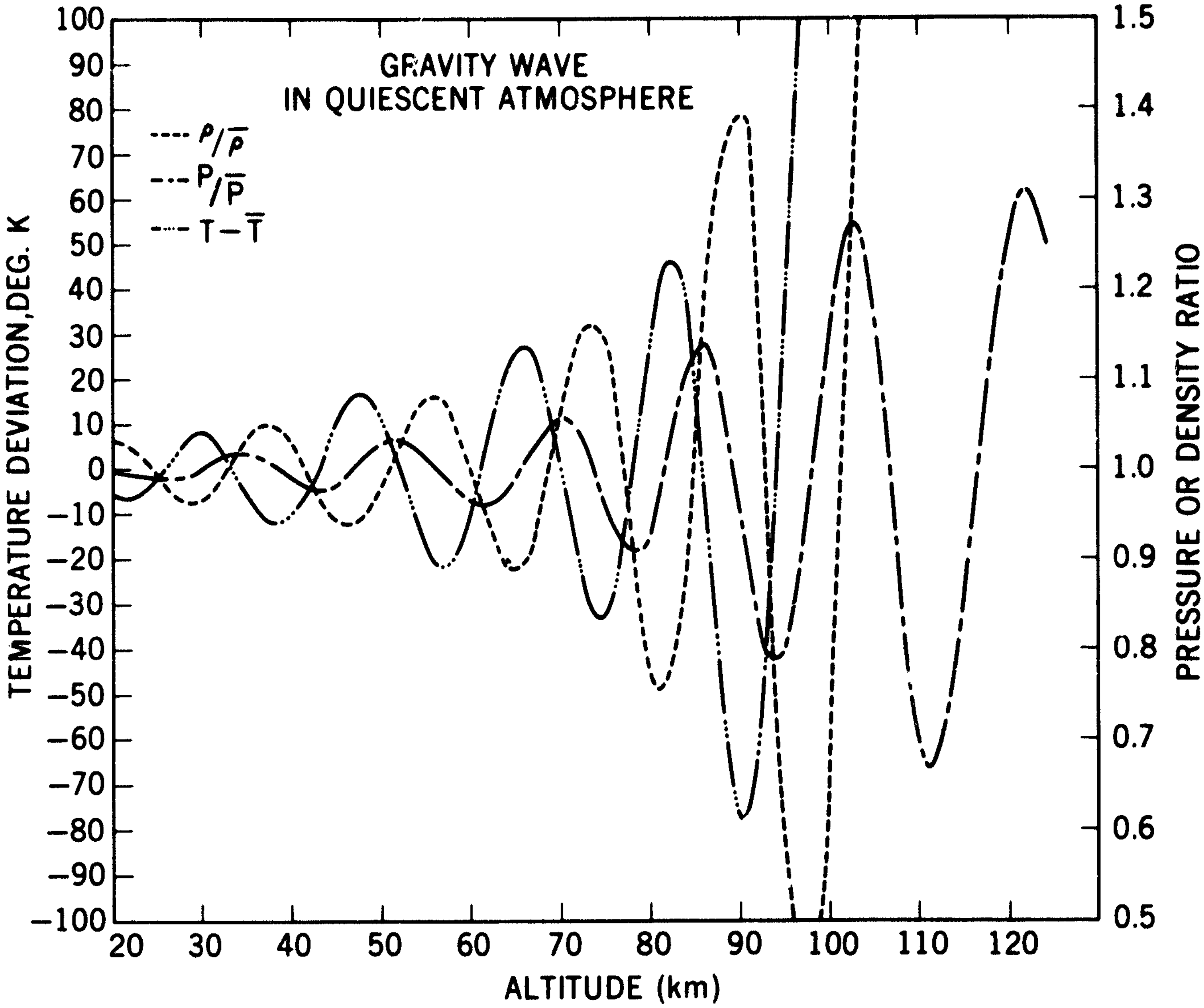

Figure 11. Calculated Gravity Wave Propagation In A Quiescent Atmosphere

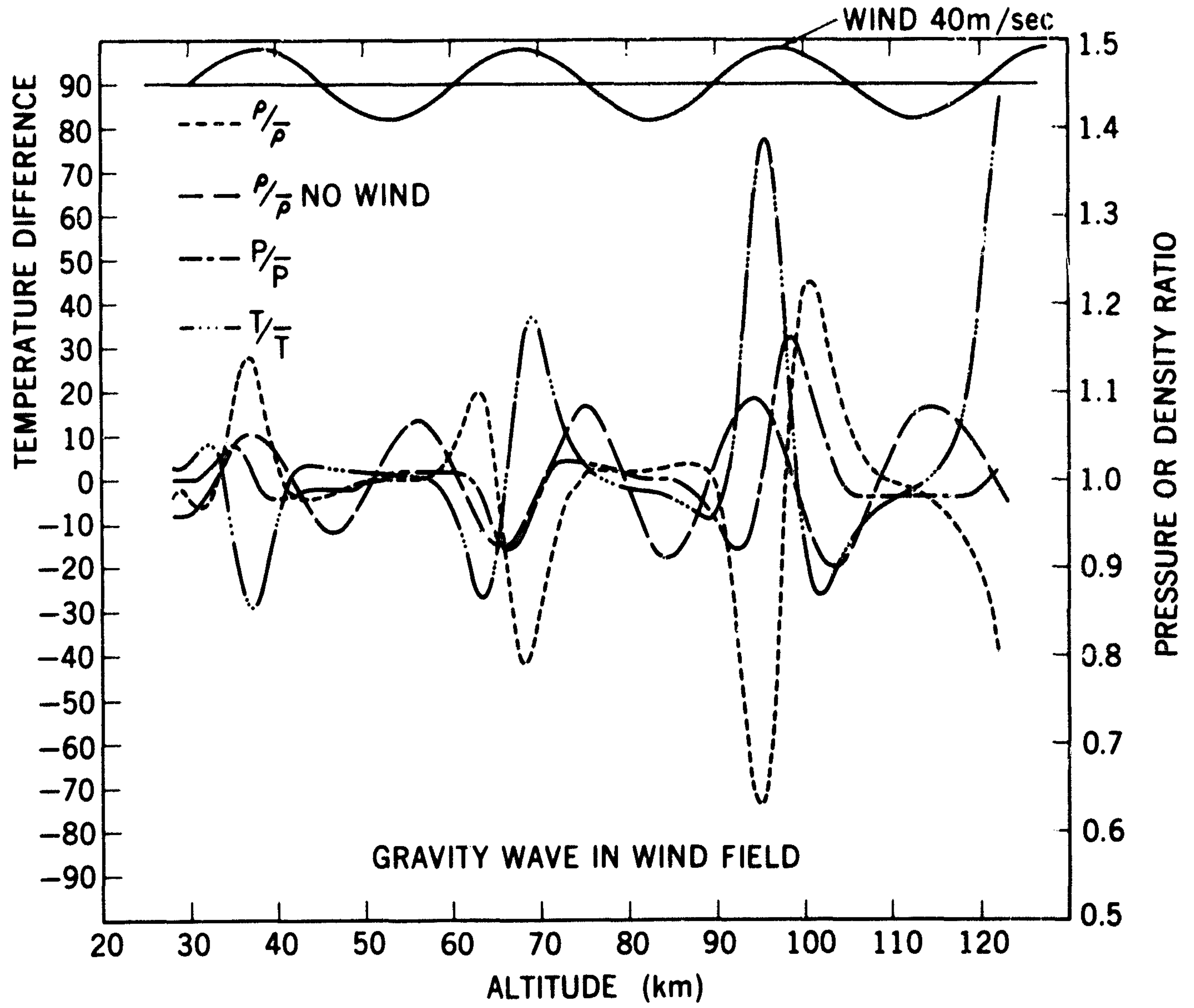

Figure 12. Calculated Gravity Wave Propagation Into A Steady Sinusoidal Wind Field

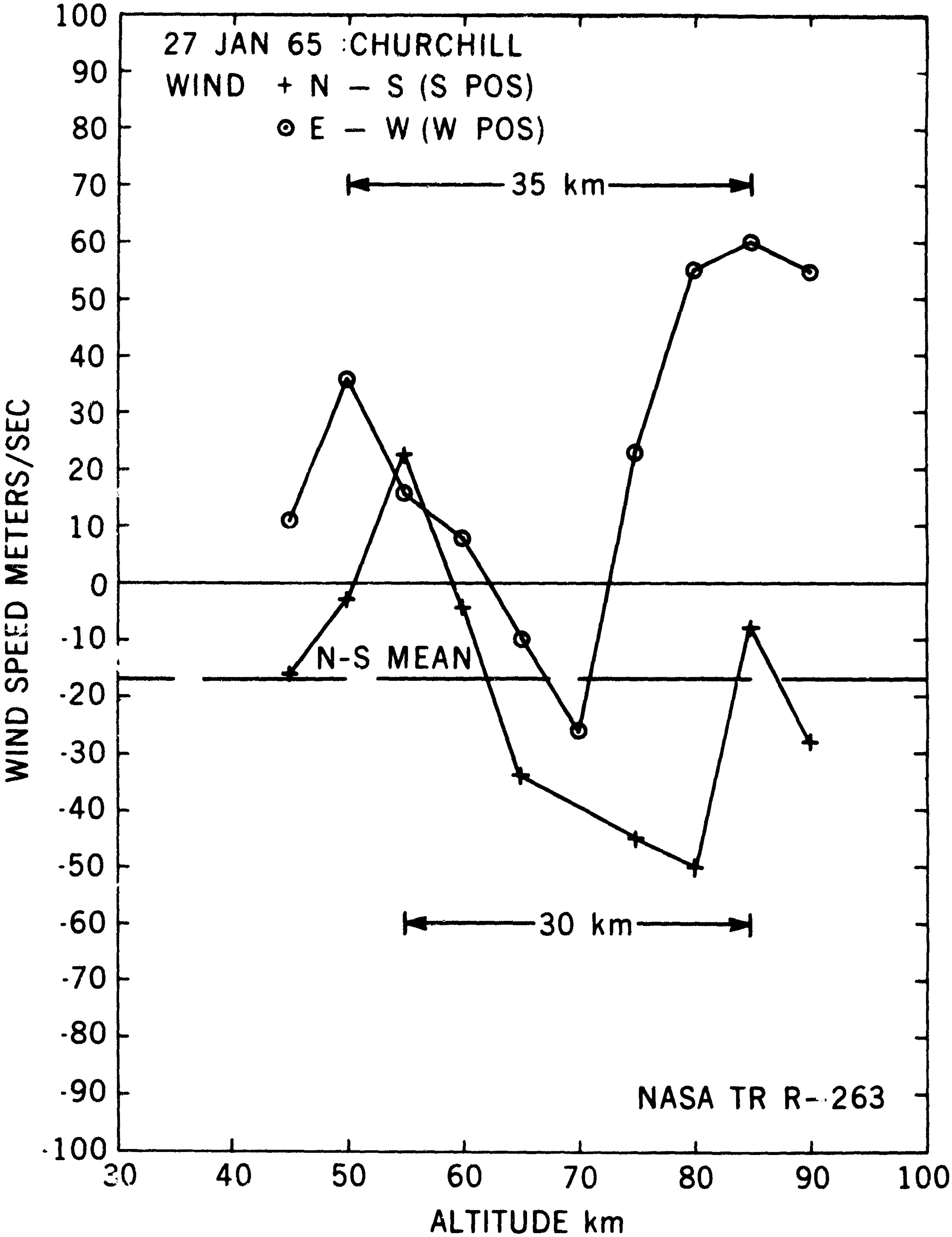

Figure 13. Observed Wind Pattern At Fort Churchill

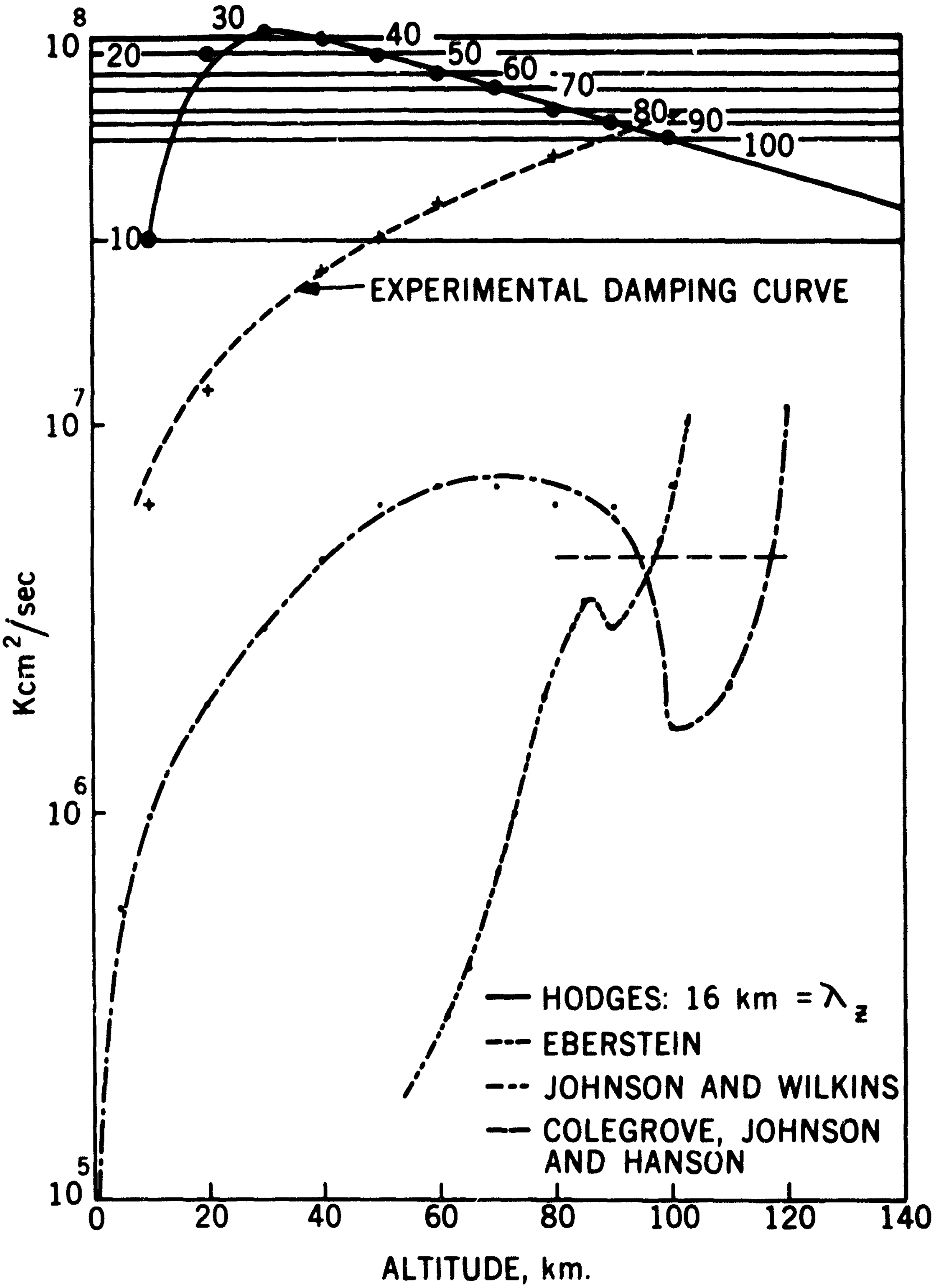

Figure 14. Estimates of Eddy Diffusivity